*Journal of Power Sources*, 46 (1993) 239–250



# Electrolyte stratification in lead/acid batteries: Effect of grid antimony and relationship to capacity loss

L. Apăteanu*, A.F. Hollenkamp** and M.J. Koop
*CSIRO Division of Mineral Products, Port Melbourne, Vic. 3207 (Australia)*

**Abstract**

Electrolyte stratification is known to cause reduced efficiency in the operation of lead/acid batteries. While this phenomenon can be clearly related to a short-term loss of performance, little is known about the effects of stratification on long-term battery usage. This issue must be considered in the more demanding types of duty, such as electric vehicle (EV) propulsion, where efficient operation for the duration of service is essential. The goal of this study has been to monitor the extent of electrolyte stratification throughout cycle life, under a repetitive deep-discharge cycling regime that typifies EV battery service. It has also been of interest to investigate any relationship between stratification and the incidence of premature capacity loss (PCL), a known cause of failure under cycling duty. We have found that cells with positive plates based on Pb–Ca and Pb–Sb positive grids both undergo an initial loss of capacity, due to the development of stratification. (Stratification disappears during the later stages of cycle life due to the extra gassing associated with the loss of capacity.) The fall in performance continues, however, through to the end of service (discharge capacity at 50% of the initial value). The relatively short cycle lives and the apparently healthy condition of plates at the end of cycling suggest that PCL, as opposed to the traditional degradation processes of grid corrosion and active-material softening/shedding, is the dominant cause of cell failure. We suggest that stratification, under our experimental regime, exerts an overall mitigating effect in the demise of the cells. The reduction in sulfuric acid concentration throughout most of the plate volume ensures that the bulk of the plate cycles in relatively weak acid: such conditions are known to reduce the severity of PCL.

## Introduction

Electrolyte stratification, as the term applies to the lead/acid battery, is best defined as the development of a vertical concentration gradient of sulfuric acid within the cell container. Stratification arises from the continual flux of acid that occurs during charge/discharge operations. The large difference in the densities of water and sulfuric acid makes possible the situation in which regions of high acid concentration (high density) become spatially resolved from regions of lower acid concentration (low density); such a situation typifies electrolyte stratification. The magnitude of stratification is readily quantified as the difference in density between electrolyte in the upper and

*On leave from the Chemical and Biochemical Energetics Institute of Bucharest, Bucharest, Romania.

**Author to whom correspondence should be addressed.

0378-7753/93/$6.00

lower zones of the active cell block and, therefore, is usually expressed in units of density (e.g., g $cm^{-3}$).

Electrolyte stratification is known to cause a loss of performance in lead/acid batteries. This has been attributed to the nonuniform utilization of plate active material that arises in a battery with stratified electrolyte [1, 2]. While this provides a clear explanation for the short-term effects of stratification, little is known about how stratification affects long-term battery service. Our interest in this area arose from research conducted in ILZRO (International Lead Zinc Research Organization) Project LE-371 on premature capacity loss (PCL) in lead/acid batteries [3–5]. During the course of this work, it was noted that certain cell configurations were associated with the establishment of persistent stratification. In addition, under a uniform experimental regime, cells based on antimony-free positive-plate grids (e.g., pure lead, lead–calcium) experienced stratification to a greater extent than did the corresponding antimony-containing cells. Given that all cells underwent capacity loss (to varying degrees) it was decided to investigate the possibility of a relationship between the two phenomena. To this end, a more detailed study of stratification was conducted, under a charge/discharge regime that was known to induce capacity loss.

## Experimental

A cell was specially designed to allow frequent measurements of electrolyte density during charge/discharge operation without causing any significant disturbance to the plate materials. An elevation view of the cell is presented in Fig. 1. As shown, the design allows for samples to be taken from nine locations across the plate group, within the separator envelope of the positive plate. The three vertical positions will be referred to as: top – T; middle – M; bottom – B. Each cell consisted of three positive and four negative plates. The central positive plate was chosen for the removal of electrolyte samples. Table 1 provides a summary of the composition of the materials that were employed in the production of the positive plates. The key plate-processing conditions are outlined in Table 2. A full description of the production methods is available elsewhere [6]. The positive-plate grids were of a light motive-power type that measured 121 mm (height) × 142 mm (width) × 3.2 mm (thickness). They were book-mould castings, produced by East Penn Manufacturing Co. (Lyon Station, PA, USA). Negative plates (of similar dimensions) were obtained in the cured state, also from East Penn Manufacturing Co. These plates were based on a Pb–Ca–(trace Sn)

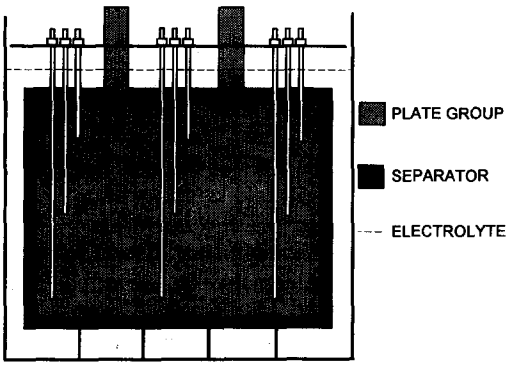


Fig. 1. Elevation view of the cell used for the measurement of electrolyte stratification.

TABLE 1

Composition of positive-plate materials

| Plate constituent | Composition |
|---|---|
| Grid | Pb–Ca: Pb–0.09wt.%Ca<br>Pb–Sb: Pb–5.7wt.%Sb–0.3wt.%Sn |
| Leady oxide | 28 wt.% Pb; 62 wt.% $\alpha$-PbO; 10 wt.% $\beta$-PbO |
| Cured material | 50 wt.% $\alpha$-PbO; 5 wt.% $\beta$-PbO; 44 wt.% $3PbO \cdot PbSO_4 \cdot H_2O$; 1 wt.% $2PbCO_3 \cdot Pb(OH)_2$ |
| Formed material | 9 wt.% $\alpha$-$PbO_2$; 86 wt.% $\beta$-$PbO_2$; 5 wt.% $PbSO_4$ |

TABLE 2

Plate-processing methods

| Production stage | Process conditions |
|---|---|
| Paste production (target: 4.1 g $cm^{-3}$) | 1400 g leady oxide, 128 ml sulfuric acid (1.40 sp. gr.), 210 $cm^3$ water, 1.1 g fibre, 1.4 g CMC[a] |
| Plate curing | 50 °C and 100% r.h. for 24 h; drying for 4 h |
| Plate formation | 72 h at 1.8 A per plate, including 2×4-h rest periods, 40 °C |

[a]CMC = carboxymethyl cellulose.

grid alloy and were used as received. When completely assembled, each cell contained ~1 $cm^3$ of 1.27 sp. gr. sulfuric acid solution per gram of positive material.

Discharge was conducted at 7.5 A (i.e., 2.5 A per positive plate) to an end-of-discharge voltage of 1.75 V (=100% depth-of-discharge (DOD)). The monitoring of plate potentials against a standard reference electrode showed that the extent of discharge was limited by the amount of electrolyte present. This was supported by calculations of the percentage utilization of the cell-active materials. Only one discharge was performed per day. The remainder of the 24-h period was devoted to charging, during which a constant current of 7.5 A was passed until the terminal voltage reached 2.55 V. This voltage was maintained until the start of the next discharge. While the specific data reported here refer to only two cells (one of each grid alloy), extensive supporting information has been gathered from other studies of similar cells [7]. The latter cells were based on the same grid alloys, but were not fitted with a device for the accurate monitoring of electrolyte density.

X-ray diffraction (XRD) analysis of the phase composition of positive-plate material was based on the output from a Philips (Eindhoven, Netherlands) model PW1710 diffractometer fitted with a Cu K$\alpha$ X-ray source. Samples were prepared as finely ground powders. Analysis for sulfur (as lead sulfate) in negative-plate material was obtained with a LECO (Michigan, USA) model CS-244 carbon and sulfur induction furnace. Sulfur was detected with an infrared detector, as sulfur dioxide. Electron microscopy was conducted with a JEOL (Tokyo, Japan) model JSM-25S III microscope that was operated at an accelerating voltage of up to 25 kV. Electron probe microanalysis was carried out on a CAMECA Camebax 'Microbeam' instrument that was operated

at an accelerating voltage of 15 kV and a beam current of 60 nA. The elements analysed, along with the respective analytical spectral lines, were: lead (M$\alpha$), sulfur (K$\alpha$), and oxygen (K$\alpha$). Raw intensity ratios were corrected for matrix effects by means of the 'PAP' matrix corrections [8]. A calibration analysis for lead and oxygen was performed on a sample of plattnerite ($PbO_2$), while sulfur analysis was standardized with data for a sample of pyrite. Prior to analysis, both standard and unknown were coated simultaneously with a thin (~20 nm) film of carbon.

## Results and discussion

Figure 2 summarizes the performance of the lead–calcium (Pb-Ca) and lead–antimony (Pb-Sb) cells, with respect to both the development of stratification and the profile of discharge capacity during cycling. Capacity loss began very early in the cycle life and was more severe for Pb–Ca than for Pb–Sb cells. After ~40 cycles, the rate of capacity loss for the former cell decreased and remained at a low level for much of the remainder of the service life. The antimonial cell maintained a higher discharge capacity. Overall, this behaviour is consistent with data that have been obtained for other, similar cells [7]. Figure 2 also shows that the electrolyte in both cells became markedly stratified within ~20 charge/discharge cycles. (Note, stratification, measured in the fully charged state, is plotted as the difference in density between the top and bottom samples.) It is clear that stratification reaches a maximum level during cycling and then falls to almost zero near the end of service. As noted in an earlier study [7], the magnitude of stratification was greater at all stages for Pb–Ca than for Pb–Sb cells.

*Stratification and effects on cell performance*

Before discussing our results in detail, it is useful to consider briefly the processes within the lead/acid cell that contribute to electrolyte stratification. Figure 3 provides a schematic representation of the key events that give rise to stratification. During discharging (Fig. 3(a)), water is liberated from the plates and moves upwards, because its density is lower than that of the surrounding electrolyte. At the electrolyte/air

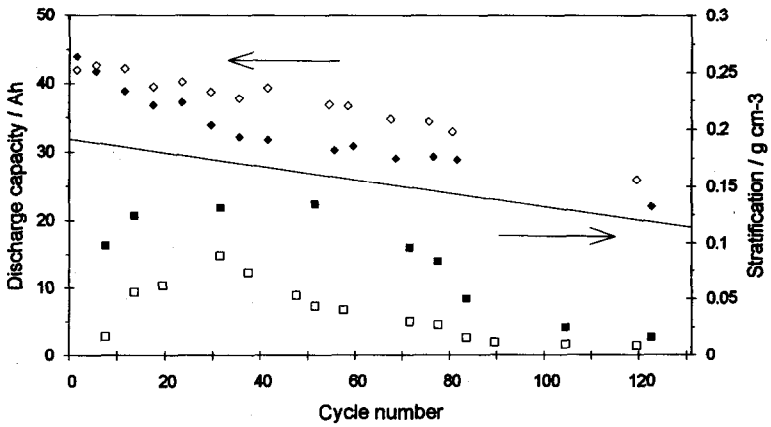


Fig. 2. Discharge capacity and stratification (at 4 h) for (◆ and ■) Pb–Ca and (◇ and □) Pb–Sb cells.

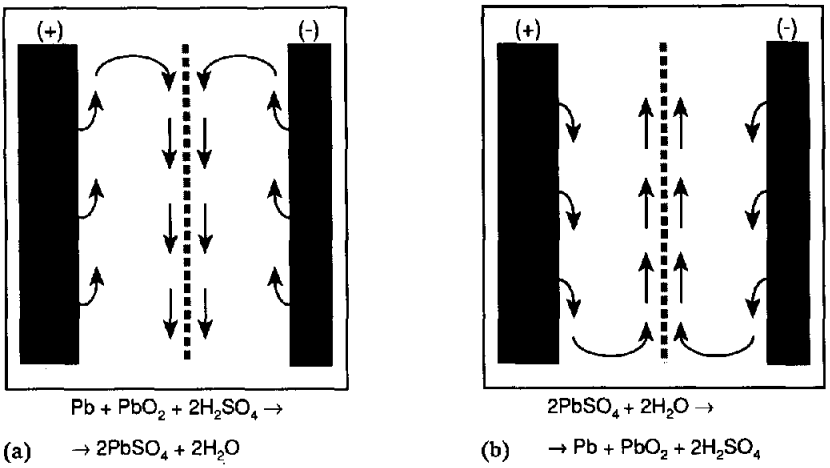


Fig. 3. Schematic of processes that contribute to stratification: (a) discharging, arrows indicate flow of water; (b) charging, arrows indicate flow of sulfuric acid.

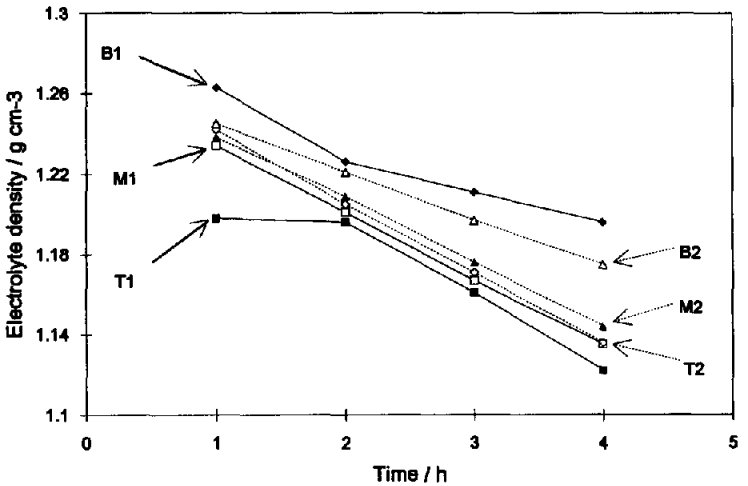


Fig. 4. Electrolyte density vs. discharge time for Pb–Ca (T1, M1, B1) and Pb–Sb (T2, M2, B2) cells at cycle no. 23.

surface, the movement of solution is redirected downwards, along the separator. Charging produces an analogous situation (Fig. 3(b)), in which sulfuric acid is liberated and moves downwards, because its density is greater than the bulk electrolyte. The 'reflection' of this movement takes place at the bottom of the cell. Detailed measurements of acid flux in lead/acid cells have been facilitated by new imaging techniques such as laser doppler velocimetry and holographic laser interferometry [9].

In our study, measurements of electrolyte density were recorded during discharge of the cells. Analysis of the data revealed stratification/cycle profiles that were similar to those plotted in Fig. 2, as well as more details on the changes in electrolyte distribution during the discharge process. The course of these changes is illustrated by Fig. 4 which presents the data obtained at cycle no. 23. First, it should be noted

that the density of the middle sample was found, in all but one instance, to be close to that of the top sample. This remained true even in situations of greatest electrolyte stratification. Clearly, stratification is seen here, not as a progressive vertical change in electrolyte density, but as a localized increase in density near the bottom of the plate. This is, in fact, a widely observed characteristic of electrolyte stratification in lead/acid batteries. Returning to Fig. 4, the results also show that differences in electrolyte density, between top and bottom samples, tend to increase during the discharge. This result is consistent with the scheme outlined in Fig. 3(a) because the movement of water upwards from the plates will increase the difference in electrolyte density between the upper and lower regions of the cell. Hence, stratification becomes greater during discharge. Figures 5 and 6 illustrate this aspect in more detail with plots of the difference in electrolyte density (top to bottom) for the Pb–Ca and the Pb–Sb cell, respectively. Significant stratification developed during the first 4 h of discharge and was more severe (~2×) for the Pb–Ca cell. For this latter cell, the data (Fig. 5) display an interesting additional feature: stratification falls to a minimum level after 1 to 2 h of discharge. This indicates that, initially, utilization of positive material is biased considerably towards that in the lower portion of the cell. Later in the discharge, this bias shifts towards the top of the cell and stratification increases.

From a thermodynamic viewpoint, the initial rate of discharge in a cell with stratified electrolyte should be greatest in the lower part of the plate, i.e., where the concentration of sulfuric acid is highest. Therefore, in the first part of discharge, sulfuric acid is consumed at a greater rate in the lower region of the cell. This reduces the magnitude of stratification, as noted above. Approaching the halfway point in the discharge, the data of Figs. 5 and 6 show clear changes in the relative rates of acid consumption in the upper and lower parts of the cell. The initial bias of discharge towards the lower region is removed and shifted to the upper region. Material utilization is now greater in the upper region of the plate and stratification increases during the remainder of the discharge. Similar results were obtained by Shimpo *et al.* [10] in their investigation of the effect of stratification on the variation of discharge rates within negative plates. This regional shift in utilization occurs as the high initial levels

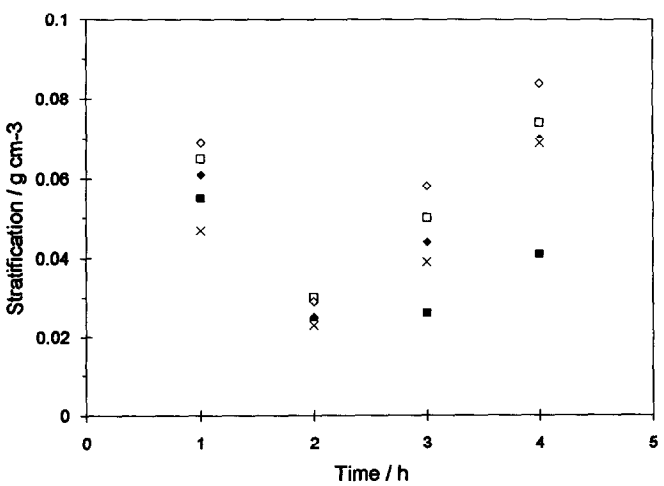


Fig. 5. Stratification vs. discharge time for Pb–Ca cell at cycle no.: (■) 5; (□) 23; (♦) 35; (◇) 55; (×) 68.

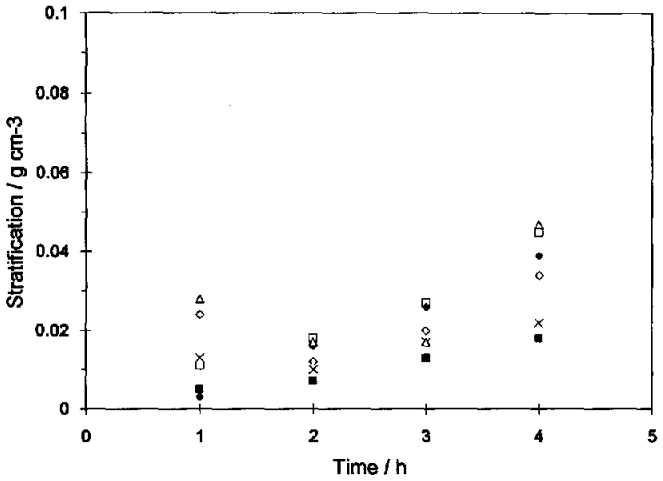


Fig. 6. Stratification vs. discharge time for Pb–Sb cell cycle no.: (■) 5; (□) 17; (♦) 23; (◇) 35; (×) 41; (△) 54.

of material utilization in the lower part of the plate lead to increased diffusion (mass transfer) polarization and hence, a reduced rate of acid consumption. In addition, any ohmic losses along the height of the plate are most likely to exert an effect during discharging, because the average resistance of the porous material increases, due to the production of lead sulfate. Both factors will decrease the rate of discharge in the lower part of the plate. This, in turn, will cause the rate of consumption of sulfuric acid in this region to fall away, relative to that in the upper region.

Finally, it is recalled from Fig. 2 that stratification disappeared late in the life of both cells. This phenomenon is readily explained by reference to the charging procedure utilized in the cycling programme. As noted earlier, the charging period is not fixed; once the discharge is finished, the remainder of the 24-h period is devoted to charging. Therefore, as the capacity of a cell drops, the charging time increases. More specifically, the portion of this time that is occupied with the electrolysis of water ('gassing') also increases. Gassing overcharge is known to be an effective way of removing electrolyte stratification. In this fashion, a steady fall in discharge capacity would be expected to cause greater and greater levels of gassing. Thus, the progressive removal of stratification is consistent with the proposed mechanism.

*Capacity loss and condition of plates*

As noted earlier, Fig. 2 showed that both cells suffered a significant loss of capacity. In fact, the data suggest a direct, qualitative relationship between stratification and capacity loss because the more severe instance of stratification (Pb–Ca) coincides with the greater decline in discharge capacity. It is noted, however, that capacity loss continued past the point at which stratification attained its highest values. Many workers have reported significant capacity loss for cells in which the electrolyte becomes stratified. According to Sunu and Burrows [1], capacity is reduced by approximately 1% for each 0.01 g $cm^{-3}$ difference in electrolyte density between the top and the bottom of the cell. This relationship serves only as a useful guide, since the actual magnitude of the capacity reduction, in specific situations, will vary with other factors such as cell geometry and the initial acid concentration. In all cases, though, the effect

of stratification is to introduce an additional mass-transfer overpotential into the operation of the cell. In other words, stratification increases the net diffusional barrier involved in the transport of sulfuric acid to the plate material. The main result is that, because of the greater overpotential, the end-of-discharge voltage is reached sooner and a reduced capacity is registered. This explanation accounts for most of the initial capacity loss during the period of increasing stratification, but it offers no obvious reason for the continued loss of capacity. To obtain more information on the cause(s) of the decline in capacity, a detailed examination of plate materials was conducted at the end of service. At that stage, the discharge capacity had fallen to close to 50% of the initial value.

Disassembly and inspection of the cells revealed that the negative plates were generally in good physical condition. Some loss of material (shedding) had occurred, but the loss was distributed uniformly over the plate. For both cells, shedding amounted to 1 to 2 wt.% of the total original negative mass. The value for the antimonial cell was slightly higher than that for the calcium cell. The positive plates also displayed varying degress of material shedding. For Pb–Sb, ~10% of the original amount of porous material was lost from the plate during cycling. More shedding was noted for the Pb–Ca cell (~20% of the original total) due to severe loss of material from the bottom part of the plate, where the concentration of sulfuric acid was highest. In particular, the three plates of this cell were all characterized by loss of complete 'pellets' of material at the bottom of the plate (i.e., grid wires were exposed).

Analysis of the phase composition, by means of XRD methods, was conducted on samples of positive material. The results are summarized in Table 3, along with those obtained in an earlier study of similar cells, cycled under the same conditions [7]. The data show that the phase composition is dominated by beta lead dioxide ($\beta$-$PbO_2$), especially for Pb–Ca cells. For Pb–Sb cells, an appreciable amount of alpha lead dioxide ($\alpha$-$PbO_2$) is also present after cycling. The third component of the plate material, lead sulfate, was present only at extremely low levels, in both types of plate. More importantly, the lead sulfate was distributed uniformly throughout each plate; it was no higher in the samples taken from the lower part of the plate. (Portions of material from the bottom of the Pb–Ca plates survived the severe shedding in that region and were, therefore, included in the analyses.) Material from the negative plates was also analysed for the presence of lead sulfate, by means of chemical analysis. The results, in Table 4, are similar to those for the positive plates in that the overall amount of lead sulfate is low (only a few wt.%). There was, however, a distinct spatial distribution of this compound: appreciably higher levels of lead sulfate were recorded, for both Pb–Ca and Pb–Sb cells, in the samples taken from the bottom of the negative plates.

TABLE 3

Phase composition (wt.%) of charged positive-plate material*

| Grid alloy | $\beta$-$PbO_2$ | $\alpha$-$PbO_2$ | $PbSO_4$ |
|---|---|---|---|
| Pb–Ca | 99 (99) | ≤1 (≤1) | ≤1 (≤1) |
| Pb–Sb | 90 (92) | 9 (7) | ≤1 (1) |

*Numbers in parentheses refer to data from the analyses of similar cells cycled in other work [7] under the same charge/discharge regime.

TABLE 4

Abundance of lead sulfate (wt.%) in samples from charged negative plates

| Sample position | Pb–Ca | Pb–Sb |
|---|---|---|
| Top left | 2.0 | 1.3 |
| Top right | 2.3 | 1.9 |
| Middle | 1.6 | 1.8 |
| Bottom left | 5.4 | 6.3 |
| Bottom right | 4.4 | 7.1 |

Several studies have shown [10, 11] that the presence of a relatively high concentration of sulfuric acid in the lower region of the cell results in an accumulation of lead sulfate in the plate material. For example, Higashimoto *et al.* [11], in their work on the cycling behaviour of valve-regulated (absorptive glass mat) lead/acid batteries, demonstrated a clear relationship between stratification, capacity loss and the accumulation of lead sulfate in the plate material near the bottom of the cells. Further, it appears that such an accumulation of lead sulfate is accentuated under conditions of inadequate charging and/or extended periods at intermediate states-of-charge [11]. It should be noted that the deposition of lead sulfate referred to in the cited reports proceeded to a much greater extent (up to 20 wt.%) than observed in the present case. The most obvious feature that accounts for this difference is the generous provision for charging in our cycling regime.

The geometry of the plates is another important factor that must be taken into consideration. Many previous studies of electrolyte stratification have concentrated on the behaviour of relatively tall cells because such a configuration is known to accentuate the phenomenon. This configuration also introduces the problem of a vertical potential drop due to the finite ohmic resistance of the plates. The use of relatively thin plates and high currents magnifies this effect. The main result of the potential drop down a plate is a reduction in material utilization in the lower parts of the plate. The processes contributing to this phenomenon have been described in considerable detail by Crennell and Lea [12]. More recently, Sunu and Burrows [1] gave an extensive account of both nonuniform current density (due to plate resistance) and electrolyte stratification in tall motive-power cells. These authors demonstrated that, depending on cell design, stratification can be greatly enhanced by ohmic effects in tall cells. In the present study, though, the plates employed cannot in any way be described as 'tall', rather, the geometry is decidedly 'oversquare', in that the width is greater than the height. This factor, combined with a relatively low rate of charge/discharge, rules out any major influence on performance by ohmic effects based on the height of the grid. In fact, evidence has been provided above that material utilization is definitely enhanced in the lower portion of the plate during the first stage of discharge. It is this aspect of cell behaviour that appears to account best for the physical degradation observed in the lower parts of plates from the more stratified (i.e., Pb–Ca) cell. In the absence of vertical ohmic effects within the plates, the relative abundance of strong sulfuric acid in the lower electrolyte volume ensures that levels of material utilization are greater near the bottom of the cell than at the top. As a result, material loss is more likely from the lower region.

Events during charging must also be considered. In cells with stratified electrolyte, it is known that the portion of a discharged plate in the strong-acid region is more

difficult to charge than the remainder. Under certain charging regimes, this may lead to overcharge factors (i.e., the ratio of charge returned to charge removed) of less than unity [10]. By comparison, the charging procedure employed in the present study was designed to ensure complete charging of the cell. This removed the possibility of undercharging and the concomitant accumulation of lead sulfate within the plate material. On the occasions that similar cells have been cycled for longer periods, extensive material loss has spread to the upper regions as well. In those cases, shedding is attributed to the enhanced grid corrosion that occurs in the zones of lower sulfuric acid concentration [13]. To investigate the incidence of grid corrosion in the present cells, samples were removed from the positive plates, at the completion of service, and were examined by scanning electron microscopy (SEM). Imaging of polished cross sections from both Pb–Ca and Pb–Sb cells yielded views that were remarkably similar. For both grid alloys, dense corrosion layers of 50 to 100 $\mu$m were found. These layers exhibited varying degrees of fracture. Analysis of elemental composition, by means of electron probe microanalysis, revealed no significant differences in composition of material in both the corrosion layer and the surrounding material. Importantly, the same uniformity was found for samples taken from the top, middle and bottom of the one plate. Thus, the presence of stratification could not be related to any chemical or morphological difference in the materials examined by electron beam methods. It seems most likely that cells were removed from service prior to the onset of severe grid corrosion.

*Reasons for cell failure*

The final aspect of the results that requires comment is the nature of the process(es) of degradation that occurred during the later stages of cycle life. It was noted above that electrolyte stratification reached a peak value within the first half of cycle life, after which it decreased to a very low level by the end of service (Fig. 2). Thus, while much of the initial capacity loss for both cells ($\sim$10% for Pb–Sb, $\sim$20% for Pb–Ca) could be attributed to stratification, this explanation could not be employed to describe cell condition at the end of service. At that point, the capacity of the Pb–Ca cell had fallen to 50% of the initial value, while the capacity of the Pb–Sb cell remained at just over 60% of the initial value. As already noted, negative plates from both cells were judged to be in good condition, at the end of service, because only minor shedding had taken place and sulfation, although unevenly distributed, amounted to only a few wt.% of the total plate mass. Therefore, an explanation for the loss of capacity must be sought in the condition of the positive plates. From earlier discussion, shedding accounts for up to 10 and 20% of the capacity loss for Pb–Sb and Pb–Ca cells, respectively. In both cells, grid corrosion and some plate distortion were also observed, although in neither case did these processes result in substantial weakening of the plates. It is reasonable, therefore, to conclude that only a very small component of the capacity loss can be associated with grid corrosion and plate distortion. A third point is the extremely low levels of lead sulfate that were found at all places within the positive plate. This rules out sulfation as a prime cause of capacity loss. Clearly, therefore, the major part of the capacity loss cannot be attributed to the well-known modes of failure in lead/acid batteries.

Finally, this discussion is concluded with a consideration of the role played by PCL in the demise of the cells. As noted earlier, no trace was found of the insulating compounds that have been implicated in the barrier-layer model of PCL [14]. Rather, the corrosion layers of all samples (antimonial and nonantimonial) were comprised of densely packed lead dioxide. The other aspect of PCL that must be considered is

the concept of a breakdown in the connectivity/conductivity of the porous active material (the so-called Kugelhaufen model [15]). Unfortunately, the acquisition of data on conductivity within the positive-plate material is, at present, problematical. It was not possible to incorporate the elaborate experimental requirements for these measurements into the present cell design. Thus, we are only able to speculate on the role of Kugelhaufen-based processes in the degradation of cell performance. Nevertheless, the absence of any clear support for the barrier-layer model (viz., layers of insulating material) provides some justification for favouring the Kugelhaufen model.

While it has not been possible to associate the observed capacity loss with any direct physical evidence, it can be stated that PCL offers the most consistent explanation of the results. The steady decline in capacity for both types of cell, faster for Pb–Ca than for Pb–Sb, agrees with recent detailed investigations of the phenomenon [7]. Stratification complicates the situation by aggravating the initial drop in performance. The effect of stratification later in cycle life is to reduce the rate of capacity loss because the separation of strong acid to the bottom of the cell means that most of the plate is cycled in a relatively weak solution of sulfuric acid. A reduction in acid concentration is known to reduce the severity of PCL [16].

## Conclusions

New detail has been provided on the relationship between capacity loss and electrolyte stratification in cells that are subjected to deep-discharge cycling duty. For both Pb–Ca and Pb–Sb grid alloys, an initial loss of discharge performance was recorded and this coincided with the development of significant stratification. The fall in performance continued, at a reduced rate, through to the end of service. During the last portion of cycle life, stratification gradually disappeared. This is related to the charging regime which delivers proportionally longer periods of overcharge as the capacity falls. The extra gassing that results is effective in mixing the regions of differing acid concentration. The observation of relatively short cycle life combined with the generally healthy condition of the positive plates suggests that PCL played a dominant role in the demise of the cells. The severity of PCL appears to be reduced by the presence of stratification because the bulk of the plate cycles in a relatively weak solution of sulfuric acid. The results have also shown that many of the deleterious effects often associated with electrolyte stratification are also dependent on the size and configuration of the cell under investigation. Thus, plates that are neither tall nor excessively thin should not suffer significant build-up of lead sulfate in the lower regions, as long as undercharging is avoided.

## Acknowledgements

The authors gratefully acknowledge support from ILZRO and useful discussions of the data with Dr D.A.J. Rand.

## References

1 W.G. Sunu and B.W. Burrows, *J. Electrochem. Soc., 128* (1981) 601.
2 J. Richter, *J. Power Sources, 42* (1993) 231.

3 K.K. Constanti, A.F. Hollenkamp, A.M. Huey and D.A.J. Rand, *ILZRO Project LE-371, Progress Rep. No. 2*, CSIRO Div. Mineral Products, Melbourne, Commun. MPC/M-256, July 1991, pp. 1–28.
4 K.K. Constanti, J.A. Hamilton, A.F. Hollenkamp, A.M. Huey and L.H. Vu, *ILZRO Project LE-371, Progress Rep. No. 3*, CSIRO Div. Mineral Products, Melbourne, Commun. MPC/M-302, Jan. 1992, pp. 1–68.
5 A.F. Hollenkamp, M.J. Koop, A.M. Huey, K.K. Constanti, J.A. Hamilton, L. Apăteanu and L.H. Vu, *ILZRO Project LE-371, Progress Rep. No. 4*, CSIRO Div. Mineral Products, Melbourne, Commun. MPC/M-349, Aug. 1992, pp. 1–58.
6 A.F. Hollenkamp, K.K. Constanti, A.M. Huey, M.J. Koop and L. Apăteanu, *J. Power Sources, 40* (1992) 125.
7 A.F. Hollenkamp, M.J. Koop, A.M. Huey, K.K. Constanti, J.A. Hamilton, L. Apăteanu and L.H. Vu, *ILZRO Project LE-371, Final Rep. (Progress Rep. No. 5)*, CSIRO Div. Mineral Products, Melbourne, Commun. MPC/M-386, Apr. 1993, pp. 1–45.
8 J.L. Pouchou and F. Pichoir, *Rech. Aerosp., 3* (1984) 167.
9 A. Eklund and R.I. Karlsson, *Electrochim. Acta, 37* (1992) 681, and references cited therein.
10 M. Shimpo, H. Nakashima, S. Sasabe and Y. Kasai, *Yuasa Jiho, 68* (1990) 26.
11 K. Higashimoto, A. Miura, T. Hayakawa and A. Komaki, *Prog. Batteries Solar Cells, 8* (1989) 268.
12 J.T. Crennell and F.M. Lea, *J. Inst. Electr. Eng., 66* (1928) 529.
13 J.J. Lander, *J. Electrochem. Soc., 98* (1951) 213.
14 A.F. Hollenkamp, *J. Power Sources, 36* (1991) 567.
15 W. Borger, U. Hullmeine, H. Laig-Hörstebrock and E. Meissner, in T. Keily and B.W. Baxter (eds.), *Power Sources 12,* International Power Sources Symposium Committee, Leatherhead, Surrey, UK, 1989, p. 131.
16 H. Nakashima and S. Hattori, *Proc. Pb80, 7th Int. Lead Conf., Madrid, Spain, May 12–15, 1980,* p. 88.